Geostationary Surface Albedo Release 2 Product Users Manual

DOI: 10.15770/EUM_SEC_CLM_0023

DOI: 10.15770/EUM_SEC_CLM_0024

DOI: 10.15770/EUM_SEC_CLM_0025

Doc.No. : EUM/OPS/REP/20/1178226
Issue : v1D e-signed
Date : 7 July 2020
WBS/DBS :

EUMETSAT
Eumetsat-Allee 1, D-64295 Darmstadt, Germany
Tel: +49 6151 807-7
Fax: +49 6151 807 555
http://www.eumetsat.int

Table of Contents

Table of Figures

Table of Tables

1 INTRODUCTION

1.1 Purpose and Scope

This document describes the Geostationary Surface Albedo (GSA) TCDR Release 2 and provides information needed to order, download, decode, and use the data. In addition, it provides summary information on the validation, including facts limiting the use of the data if there are any.

1.2 Applicable Documents

AD1	The Meteosat Surface Albedo Climate Data Record Validation Report (Release 1)	EUM/OPS/REP/13/726421
AD2	Meteosat Surface Albedo Retrieval: Algorithm Theoretical Basis Document	EUM/OPS/SPE/12/3367
AD3	Geostationary Surface Albedo (GSA) Release 2 Validation Report	EUM/CLIMATE/REP/19/1153696
AD4	NetCDF Creation Guidelines; Best Practises, Conventions and Applicable Standards	EUM/OPS/STD/11/3120

1.3 Reference Documents

RD1.	Wang, Z., Schaaf, C., Lattanzio, A., Carrer, D., Grant, I., Román, M., Camacho, F., Yu, Y., Sánchez-Zapero, J. & Nickeson, J. (2019). Global Surface Albedo Product Validation Best Practices Protocol. Version 1.0. In Z. Wang, J. Nickeson & M. Román (Eds.), Best Practice for Satellite Derived Land Product Validation (p. 45): Land Product Validation Subgroup (WGCV/CEOS). DOI:10.5067/DOC/CEOSWGCV/LPV/ALBEDO.001
RD2.	GCOS-92 (2004), Implementation Plan For The Global Observing System For Climate In Support Of The UNFCCC.
RD3.	Lattanzio, A.,Y.Govaerts, and B.Pinty (2006). Consistency of surface anisotropy characterization with Meteosat observations. Advanced Space Research, doi:10.1016/j.asr.2006.02.049.
RD4.	Govaerts, Y., and Lattanzio, A. (2007). Retrieval Error Estimation of Surface Albedo Derived from Geostationary Large Band Satellite Observations: Application to Meteosat-2 and -7 Data. Journal of Geophysical Research 112, doi:10.1029/2006JD007313
RD5.	Pinty, B., F. Roveda, M.M. Verstraete, N. Gobron, Y. Govaerts, J.V. Martonchik, D.J. Diner, and R.A. Kahn (2000a). Surface albedo retrieval from Meteosat: Part1: Theory. Journal of Geophysical Research 105, 18099–18112.
RD6.	Pinty, B., F. Roveda, M.M. Verstraete, N. Gobron, Y. Govaerts, J.V. Martonchik, D.J. Diner, and R.A. Kahn (2000b). Surfaceal bed or retrieval from Meteosat: Part 2: Applications Journal of Geophysical Research 105, 18113–18134.
RD7.	Algorithm Theoretical Basis Document Meteosat Cloud Fractional Cover (COMET) Edition 1, 2017. DOI: 10.5676/EUM SAF CM/CFC METEOSAT/V001
RD8.	Loew, A. and Govaerts, Y.: Towards multidecadal consistent meteosat surface albedo time series, Remote Sens., 2, 957–967. DOI:10.3390/rs2040957, 2010.
RD9.	Y. M. Govaerts, B. Pinty, M. Taberner, A. Lattanzio, "Spectral conversion of surface albedo derived from meteosat first generation observations", IEEE Geosci. Remote Sens. Lett., vol. 3, pp. 23-27, Jan. 2006.

RD10.	Lattanzio, A.; Schulz, J.; Matthews, J.; Okuyama, A.; Theodore, B.; Bates, J.J.; Knapp, K.R.; Kosaka, Y.; Schüller, L. Land Surface Albedo from Geostationary Satelites: A Multiagency Collaboration within SCOPE-CM. Bull. Amer. Meteorol. Soc 2013, 94, 205–214. DOI: 10.1175/BAMS-D-11-00230.1
RD11.	Loew, A., Bennartz, R., Fell, F., Lattanzio, A., Doutriaux-Boucher, M., and Schulz, J.: A database of global reference sites to support validation of satellite surface albedo datasets (SAVS 1.0), Earth Syst. Sci. Data, 8, 425-438. DOI:10.5194/essd-8-425-2016
RD12.	Dee et al., The ERA-Interim reanalysis: configuration and performance of the data assimilation system, https://doi.org/10.1002/qj.828, QJRMet, 2011.
RD13.	Lattanzio, A., Fell, F., Bennartz, R., Trigo, I. F., and Schulz, J.: Quality assessment and improvement of the EUMETSAT Meteosat Surface Albedo Climate Data Record, Atmos. Meas. Tech., 8, 4561–4571. DOI: 10.5194/amt-8-4561-2015, 2015
RD14.	Diner, D. J., W. A. Abdou, A. T. P., K. Crean, H. R. Gordon, R. A. Kahn. J. V. Martonchik, S. R. Paradise, B. Pinty, M. M. Verstraete, M. Wang, and R. A. West (1997). *MISR Level 2 Aerosol Retrieval Algorithm Theoretical Basis. Technical Report* JPL D-11400, Rev. C, NASA, Jet Propulsion Laboratory.
RD15.	Govaerts, Y. M., Lattanzio, A., Taberner, M. and Pinty, B.: Generating global surface albedo products from multiple geostRD10ationary satellites, Remote Sensing of Environment, 112(6), 2804–2816, doi:10.1016/j.rse.2008.01.012, 2008.

1.4 Acronyms and abbreviations

AOT	Aerosol Optical Thickness
API	Application Programming Interface
ASM	Atmosphere Scattering Module
ATBD	Algorithm Theoretical Basis Document
BHR	Bi-Hemispherical Reflectance
BHRiso	BHR under perfect isotropic illumination conditions (or WSA)
BRDF	Bidirectional Reflectance Distribution Function
BSA	Black Sky Albedo (or DHR)
CFC	Cloud Fractional Cover
CLM	CLoud Mask
CSDP	Climate Service Development Plan
DAM	Data Accumulation Module
DOI	Digital Object Identifier
ECMWF	European Centre for Medium-range Weather Forecasts
GSA	Geostationary Surface Albedo
HDF	Hierarchical Data Format
IODC	Indian Ocean Data Coverage
JRC	Joint Research Centre
MARF	Meteorological Archive Retrieval Facility
MPEF	Meteorological Product Extraction Facility
MSA	Meteosat Surface Albedo
MVIRI	Meteosat Visible and Infrared Imager
RPV	Rahman-Pinty-Verstraete
RTM	Radiative Transfer Model
SAM	Space Averaging Module
SEVIRI	Spinning Enhanced Visible and Infrared Imager

SSR	Sensor Spectral Response
TAM	Space-Time Averaging Module
TCDR	Thematic Climate Data Record
TCO3	Total Column Ozone
TCWV	Total Column Water Vapour
TOA	Top Of Atmosphere
UMARF	Unified Meteorological Archive and Retrieval Facility
VIS	Visible
WSA	White Sky Albedo (or BHRiso)

2 DATA RECORD OVERVIEW

General	Data record name	Geostationary Surface Albedo Release 2
	Data record digital identifier	DOI: 10.15770/EUM_SEC_CLM_0023 (0-degree) DOI: 10.15770/EUM_SEC_CLM_0024 (57-degree) DOI: 10.15770/EUM_SEC_CLM_0025 (63-degree)
	Data record short description	Second release of the TCDR of surface albedo from Meteosat first and second generation
	Record type	Thematic Climate Data Record
	Content	Meteosat Level 2 black-sky and white-sky albedo with uncertainty estimates
Coverage	Spatial	• Meteosat disk – land surface • each pixel (IFOV) ground resolution of 2.5 km (3.0 km) for MVIRI (SEVIRI) at sub-satellite point.
	Time period	01 January 1982 – 31 December 2017
	Temporal frequency	10 day composite
Instrument	Instruments names	Meteosat Visible and Infrared Imager (MVIRI) Spinning Enhanced Visible and Infrared Imager (SEVIRI)
	Instruments descriptions	**MVIRI** is a passive imaging radiometer, the optical system consists of a scanning Ritchey-Chretien telescope with a primary aperture of 400 mm diameter (140 mm secondary aperture) and focal lengths of 3650 mm for VIS (resolution 2.5 km) and 535 mm for WV and IR ranges (resolution 5 km). **SEVIRI** is a compact telescope and scan assembly, allowing the implementation of a large passive cooler which improves IR detector performances by lowering their operating temperature. The imaging SEVIRI radiometer is equipped with a patented three-mirror (3M) telescope of compact design (focal length of 5367 mm) which allows the insertion of a small black body for full-pupil calibration. It has 12 spectral channels, 11 provide measurements with a resolution of 3 km at the sub-satellite point. The twelfth, so-called HRV (High Resolution Visible) channel of SEVIRI (Spinning Enhanced Visible and Infrared Imager), provides measurements with a resolution of 1 km.
Instrument Data	Input data	MVIRI/SEVIRI Level 1.5 ERA-Interim TCWV and TCO3 Cloud Mask
	Output data	Meteosat Level 2 black-sky and white-sky albedo with uncertainties
	Format	NetCDF4
Access	EUMETSAT Data Centre	The data set is available from EUMETSAT Data Centre (https://eoportal.eumetsat.int/)
	Delivery	• ftp push • online pull

3 DATA RECORD DEFINITION

3.1 Temporal and spatial coverage

Geostationary land surface albedo is derived exploiting imagery acquired from the Meteosat Visible and Infrared Imager (MVIRI) on board Meteosat First Generation (MFG) and the Spinning Enhanced Visible and Infrared Imager (SEVIRI) onboard Meteosat Second Generation (MSG). It provides 10-day composite products derived over the full disk, with maximum extents of 65°N − 65°S and 65°W − 65°E around the nominal Sub-Satellite Point (SSP) (see Figure 1). The current release contains improvements and spatial-temporal extensions compared to the first release [AD1]. The Meteosat imagery has been processed with the GSA algorithm developed by EUMETSAT that is an extension of the original Meteosat Surface Albedo (MSA) software developed at the Space Applications Institute of the Joint Research Centre (JRC) of the European Commission.

Satellite	Instrument/Channel	Mission (SSP)	Start Date	End Date
Meteosat-2	MVIRI/VIS	0DEG (0°)	1981-08-16	1988-08-11
Meteosat-3	MVIRI/VIS	0DEG (0°)	1988-08-11	1991-01-25
Meteosat-4	MVIRI/VIS	0DEG (0°)	1989-06-19	1994-02-04
Meteosat-5	MVIRI/VIS	0DEG (0°)	1991-05-02	1997-02-13
		IODC (63°E)	1998-07-01	2007-04-16
Meteosat-6	MVIRI/VIS	0DEG (0°)	1996-10-21	2000-01-20
Meteosat-7	MVIRI/VIS	0DEG (0°)	1998-06-03	2006-07-19
		IODC (57°E)	2006-11-01	2017-03-31
Meteosat-8	SEVIRI/HRV	0DEG (0°)	2004-03-01	2007-05-31
Meteosat-9	SEVIRI/HRV	0DEG (0°)	2007-05-01	2013-04-30
Meteosat-10	SEVIRI/HRV	0DEG (0°)	2013-04-01	2017-12-31

Table 1: Satellite, instrument, mission, nominal orbit position and services for the period 1981-2017. The period includes Meteosat 2-7 (MFG) and Meteosat 8-10 (MSG).

The temporal coverage (see Table 1) of the data record is more than 36 years for the Prime mission at 0° longitude (see Figure 1). For the IODC mission, the temporal coverage is close to 20 years. Some gaps are present, due to missing satellite images. It is important to highlight that a minimum of six daylight and cloud-free observations for each day are necessary to retrieve the albedo variables. A comprehensive view of the gaps in the time series is presented in Appendix A.

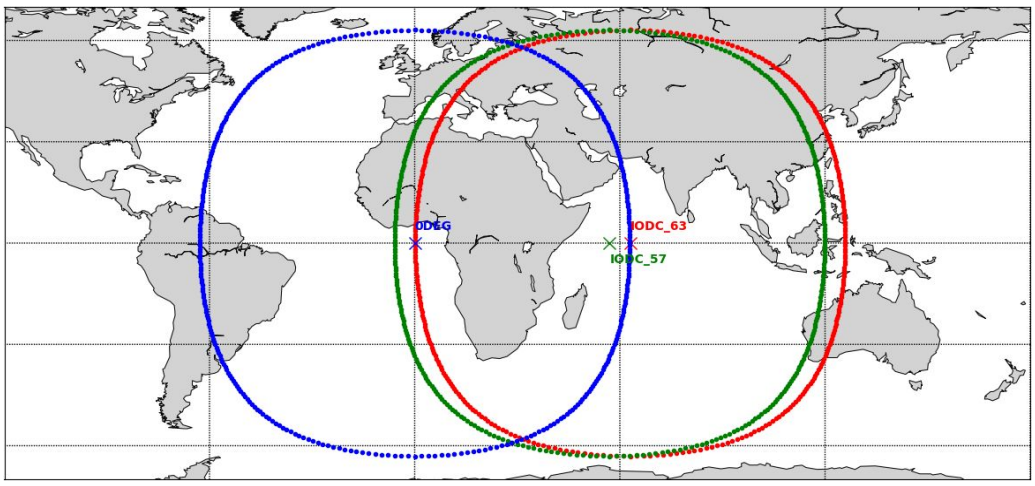

Figure 1: 0DEG (in blue), IODC (57E in green and 63E in red) spatial coverage.

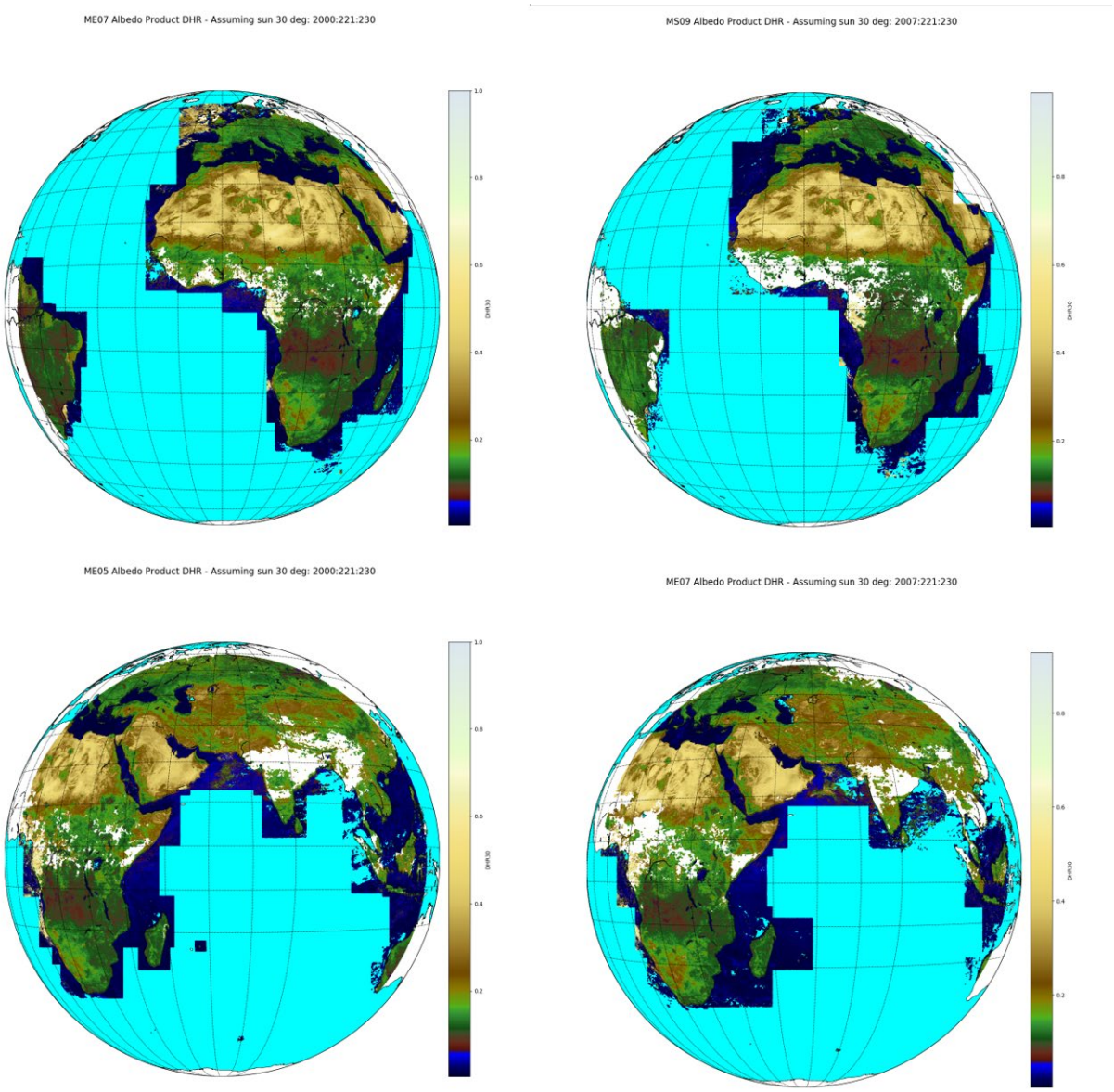

Figure 2: Example DHR30 from GSA: MET7@0000 (upper left), MET09@0000 (upper right), MET05@0630 (lower left) and MET07@0570 (bottom right)

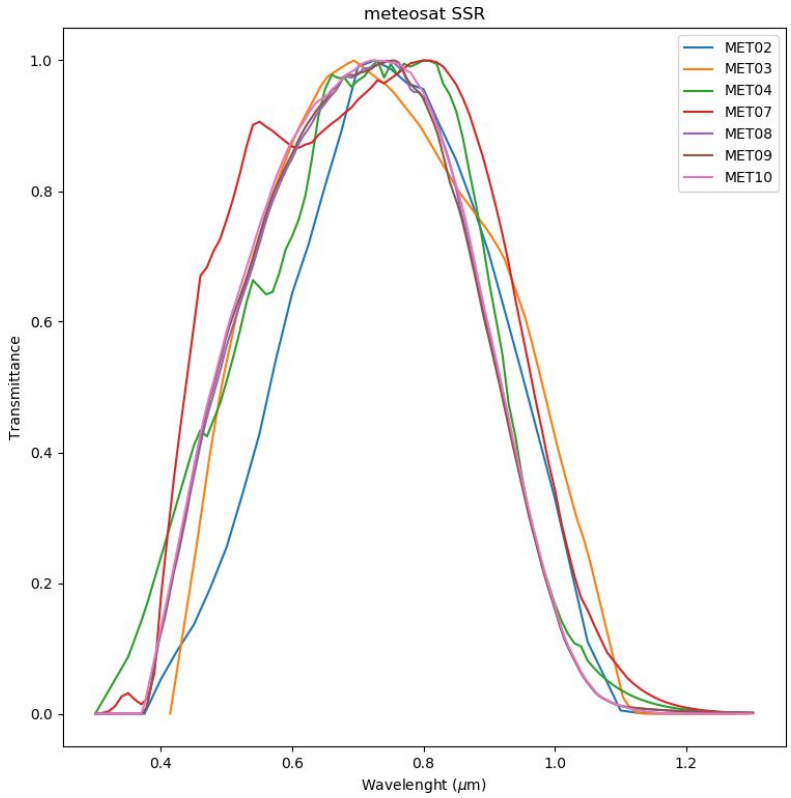

Figure 3: Sensor Spectral Response (SSR) for the VIS (HRV) band of MVIRI (SEVIRI)

3.2 Albedo quantities in the data record

The following definitions, from [RD1], clarify the physical meaning of the different variables, measurable from satellite observations, describing the land surface albedo.

- **Black-Sky Albedo (BSA):** Black-sky albedo or Directional Hemispherical Reflectance (DHR) is the albedo in the absence of any diffuse irradiance component (no atmospheric scattering), with only a direct illumination component. The Global Climate Observing System (GCOS) implementation plan [RD2] specifies that the black-sky albedo is the product required for climate change purposes.

- **White-Sky Albedo (WSA):** White-sky albedo or bi-hemispherical albedo under isotropic illumination (BHR_{iso}) is the albedo in the absence of any direct illumination component but only comprised of isotropic diffuse illumination. This component is sensitive to the intrinsic coupling between the surface and the scattering atmosphere.

The retrieval is performed using the spectral instrument visible channel (VIS) for MVIRI (Meteost-2 to Meteosat-7) and in the High-Resolution Visible (HRV) channel for SEVIRI (Meteosat-8 to Meteosat-10). The product contains also the uncertainties and other ancillary information (see Section 6).

Figure 3 shows the spectral bands for the individual instruments giving an indication how diverse they are. In order to make the albedo estimates comparable and enable comparison with other surface albedo data records, the albedo quantities retrieved with GSA should be converted into a

broadband spectral interval (0.3-3.0 µm). The complete list of coefficients for calculating broadband albedo estimates from the spectral retrieved quantities is provided in Section 3.3.

3.3 Conversion to Broadband albedo

The method transforms the DHR/BHRiso derived in the Meteosat VIS band $(DHR/BHRiso)_{VIS,}$ in shortwave broadband albedo $(DHR/BHRiso)_{BB}$. The conversion to broadband is done for MVIRI (Meteosat-2 to Meteosat-4) following the procedure given in [RD8] and for MVIRI (Meteosat-5 to Meteosat-7) and SEVIRI following the method as described in [RD9]. The different approach applied to the first three MVIRI instruments is due to an issue in the Sensor Spectral Response (SSR) provided that leads to temporal discrepancies. For this reason, Loew and Govaerts developed an empirical method to derive the spectral coefficients for the Meteosat-2 to Meteosat-4 satellites ([RD8]). The relation between spectral and broadband is the same in both cases and is described by a third-order polynomial written as follows:

$$VAR_{BB} = a + bVAR_{VIS} + c(VAR_{VIS})^2 + d(VAR_{VIS})^3 \quad \text{Equation 1}$$

where VAR is either DHR or BHRiso, each using a different set of conversion coefficients *a–d* for the DHR (Table 2) and BHRiso (Table 3) per Meteosat satellite.

Met	a	b	c	d
2	-2.95364443e-05	1.22636437e+00	-1.45464587e+00	1.27798259e+00
3	-2.95364443e-05	1.32036722e+00	-1.52968502e+00	1.25365901e+00
4	-2.95364589e-05	1.22655797e+00	-1.07426369e+00	8.96015048e-01
5	-2.95364443e-05	1.25341415e+00	-1.09384084e+00	8.89843404e-01
6	-2.95364443e-05	1.30573940e+00	-1.31526375e+00	1.05711114e+00
7	-2.95364589e-05	1.26273489e+00	-1.11476350e+00	9.00940299e-01
8	-5.87700000e-03	1.53323200e+00	-2.61389100e+00	2.89949100e+00
9	-5.99900000e-03	1.56889600e+00	-2.75666500e+00	3.11088200e+00
10	-6.02100000e-03	1.56626500e+00	-2.74375400e+00	3.09211000e+00

Table 2: Empirical coefficients a–d for the DHR conversion

Met	a	b	c	d
2	-2.85976712e-05	9.81895685e-01	-8.48408699e-01	7.43798614e-01
3	-2.85976712e-05	1.09896255e+00	-1.07471538e+00	9.11732554e-01
4	-2.85976712e-05	1.00361478e+00	-6.55005634e-01	6.47315860e-01
5	-2.85976712e-05	1.04928327e+00	-7.66418219e-01	7.47902989e-01
6	-2.85976712e-05	1.15992260e+00	-1.13301563e+00	9.98916626e-01
7	-2.85976712e-05	1.03751910e+00	-6.88233614e-01	7.00615168e-01
8	-1.61670000e-02	1.63337800e+00	-2.99600600e+00	3.27934400e+00
9	-1.62780000e-02	1.67045700e+00	-3.14845100e+00	3.50383800e+00
10	-1.63290000e-02	1.66796800e+00	-3.13584200e+00	3.48480100e+00

Table 3: Empirical coefficients a–d for the BHRiso conversion

3.4 BHRiso Uncertainty Estimation

The DHR uncertainty is part of the GSA product, while the BHR_{iso} is currently not. The latter can be calculated with the following expression:

$$\sigma_{BHR_{iso}} = \sqrt{\sigma_{\rho_0}^2 + (\frac{\delta_{\alpha_0}(\hat{k},\hat{\Theta})}{\delta k}\sigma_{\hat{k}})^2 + (\frac{\delta_{\alpha_0}(\hat{k},\hat{\Theta})}{\delta \Theta}\sigma_{\hat{\Theta}})^2}$$

Equation 2

$\sigma_{\bar{k}}$ is the retrieved uncertainty of the parameter k
$\sigma_{\bar{\Theta}}$ is the retrieved uncertainty of the parameter Θ
Where α_0 (see [RD5]) is tabulated with the following value:

h	Θ	k	α_0	h	Θ	k	α_0
0.15	-0.30	0.40	3.29568	0.15	-0.15	0.80	1.87455
0.15	-0.30	0.50	2.91138	0.15	-0.15	0.90	1.74369
0.15	-0.30	0.60	2.62286	0.15	-0.15	1.00	1.63808
0.15	-0.30	0.70	2.40092	0.15	-0.10	0.40	2.74655
0.15	-0.30	0.80	2.22700	0.15	-0.10	0.50	2.39410
0.15	-0.30	0.90	2.08885	0.15	-0.10	0.60	2.12919
0.15	-0.30	1.00	1.97802	0.15	-0.10	0.70	1.92501
0.15	-0.25	0.40	3.15165	0.15	-0.10	0.80	1.76452
0.15	-0.25	0.50	2.77600	0.15	-0.10	0.90	1.63641
0.15	-0.25	0.60	2.49365	0.15	-0.10	1.00	1.53294
0.15	-0.25	0.70	2.27618	0.15	-0.05	0.40	2.61871
0.15	-0.25	0.80	2.10550	0.15	-0.05	0.50	2.27346
0.15	-0.25	0.90	1.96964	0.15	-0.05	0.60	2.01425
0.15	-0.25	1.00	1.86037	0.15	-0.05	0.70	1.81463
0.15	-0.20	0.40	3.01252	0.15	-0.05	0.80	1.65780
0.15	-0.20	0.50	2.64497	0.15	-0.05	0.90	1.53264
0.15	-0.20	0.60	2.36857	0.15	-0.05	1.00	1.43151
0.15	-0.20	0.70	2.15551	0.15	0.00	0.40	2.49373
0.15	-0.20	0.80	1.98812	0.15	0.00	0.50	2.15556
0.15	-0.20	0.90	1.85469	0.15	0.00	0.60	1.90210
0.15	-0.20	1.00	1.74715	0.15	0.00	0.70	1.70718
0.15	-0.15	0.40	2.87767	0.15	0.00	0.80	1.55420
0.15	-0.15	0.50	2.51782	0.15	0.00	0.90	1.43218
0.15	-0.15	0.60	2.24720	0.15	0.00	1.00	1.33363
0.15	-0.15	0.70	2.03856				

Table 4: α_0 according to RPV parameters allowed values.

4 QUALITY OF RELEASE 2

The quality analysis has been divided into three main parts: (1) the assessment of the improvement due to the usage of an external cloud mask compared with the previous release, (2) a consistency analysis on the overlap region (see Figure 1), and (3) a comparison against reference data records.

4.1 Improvement compared to Release 1

Release 1 is referred to Meteosat Surface Albedo (MSA), while Release 2 to Geostationary Surface Albedo (GSA). The retrieval core is the same but GSA has an extra processing layer allowing the application to any Geostationary satellite [RD10], while MSA only allowed to process Meteosat First Generation imagery.

Two immanent improvements are that the time series of GSA Release 2 is significantly longer by making the GSA retrieval applicable to Meteosat Second Generation data and the extension of the product spatial coverage that includes now the part of South America covered by the Meteosat 0° longitude mission.

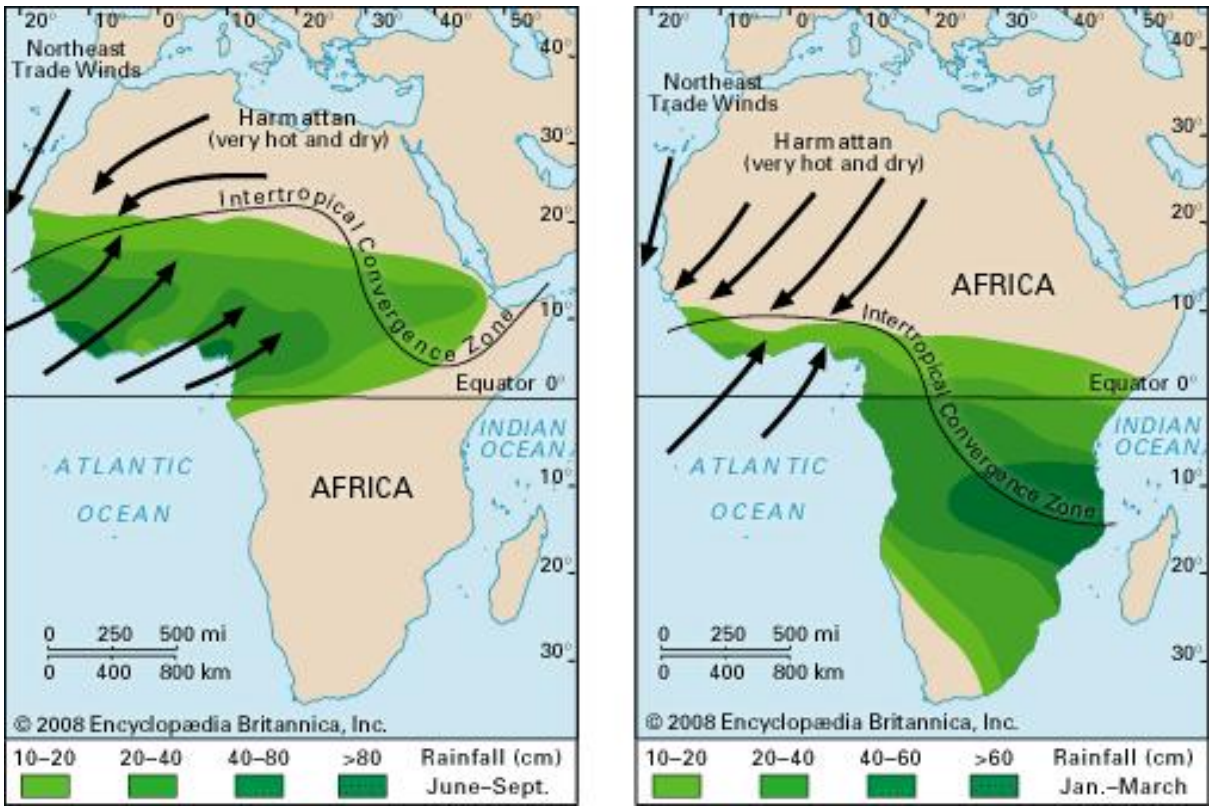

Figure 4: Seasonal distribution of precipitations due to the ITCZ shift and African Monsoon (Picture Credits: Climate and Ocean: Variability, Predictability and Change (CLIVAR))

The main improvement of GSA Release 2 compared to Release 1 is the exploitation of an external cloud mask (see Section 5.1.2). The not removed cloud contamination was the most relevant factor affecting the quality of Release 1 [AD1]. In order to verify that the cloud contamination in this release has decreased, two regions are analysed. The precipitation regime in these regions (and the cloud coverage) is known to depend on the shift of the Intertropical Convergence Zone (ITCZ) and the African Monsoon[1]. More precipitation is expected north of the Equator from June to September, and south of the Equator from January-March (see Figure 4). Because the level of precipitation is connected with the cloud amount and its temporal persistence, the impact of using or not an external cloud mask should show a clear signature. In order to check the presence of such a signature, the

[1] Source: Climate and Ocean: Variability, Predictability and Change (CLIVAR) http://www.clivar.org/african-monsoon (Link valid 15/03/2020)

Release 1 and Release 2 DHR30 values retrieved over two regions; one north and one south of the Equator have been compared for the year 2001.

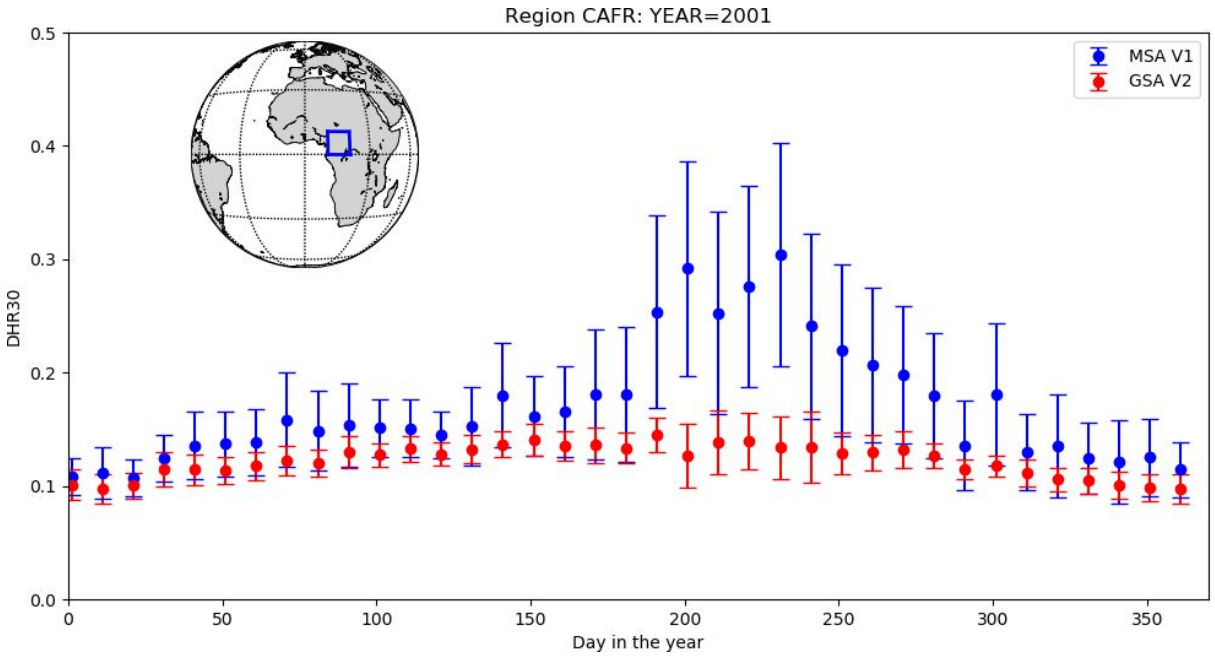

Figure 5: Comparison of DHR30 values as retrieved in the displayed region for MSA Release 1 (blue) and GSA Release 2 (red).

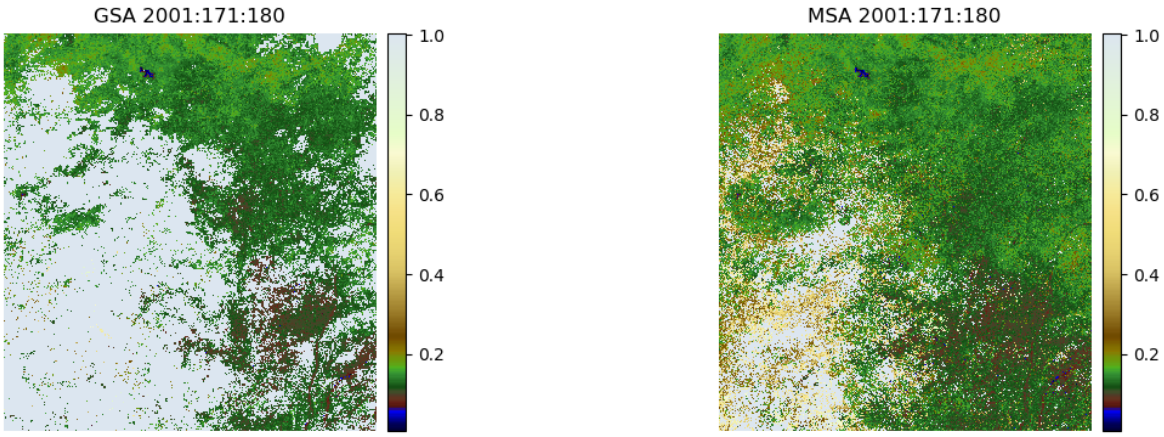

Figure 6: Map comparison of DHR30 values between GSA Release 2 (left panel) and MSA Release 1 (right panel) for the period 171-180 (20th to 30th of June) 2001.

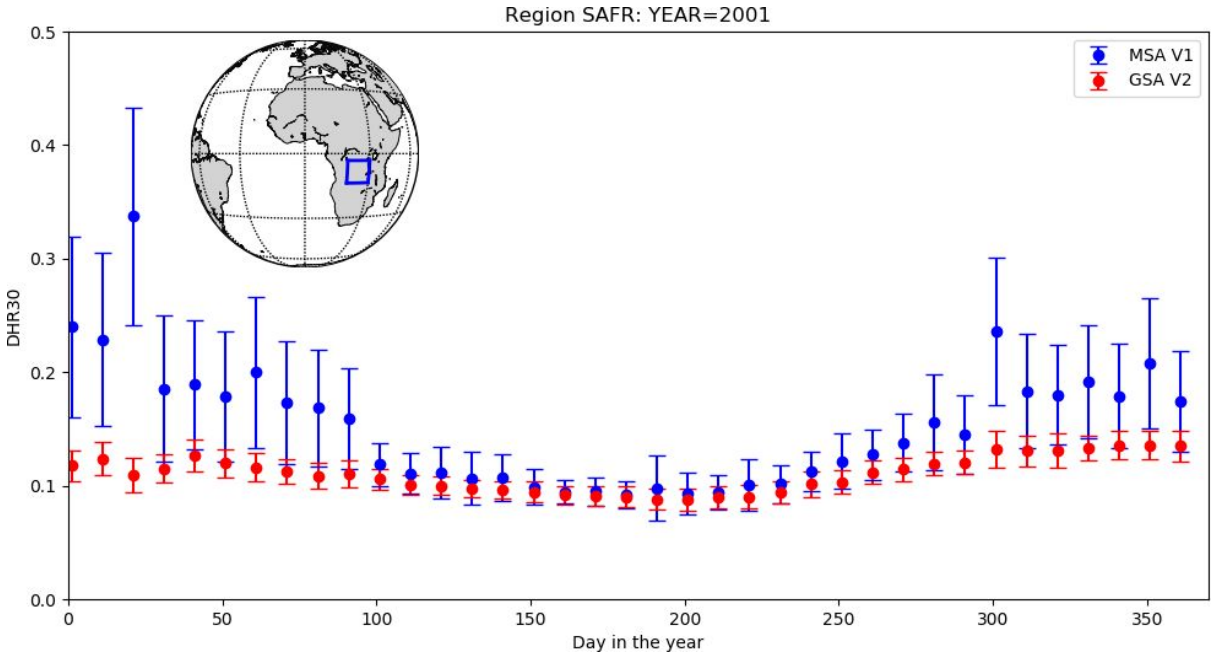

Figure 7: Comparison of DHR30 values as retrieved in the displayed region for MSA Release 1 (blue) and GSA Release 2 (red).

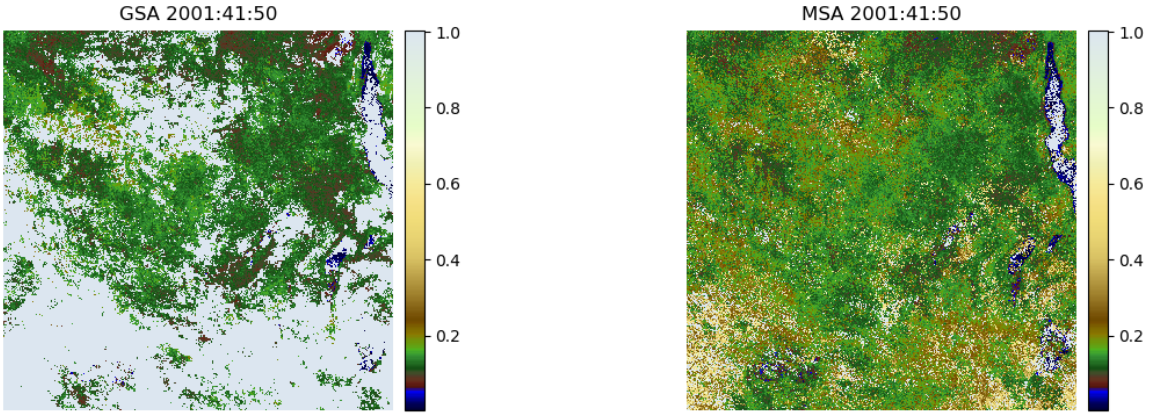

Figure 8: Map comparison of DHR30 values between GSA Release 2 (left panel) and MSA Release 1 (right panel) for the period 041-050 (10th to 20th of February) 2001.

The impact of detecting clouds more effectively is clearly visible in the period June-September north of the Equator (see Figure 5 and Figure 6) and in the period January-March south of the Equator (see Figure 7 and Figure 8). As expected, the exploitation of an external cloud mask removes the signature of clouds in the albedo fields. This is resulting in a smaller number of albedo estimates by removing unrealistically high albedo values leading to a reduction of a spurious temporal variability. The remaining retrieved values will have higher reliability and quality.

4.2 Validation summary

The GSA product was validated using external reference data [AD3]. The data record shows very good stability over the full time period, both looking at the overall Meteosat disk average and at the validation sites. The decadal trend is less than 1% for most sites. The only exception is the urban site MONGU in southern Africa. However, this site by definition (urban site) is not supposed to show a stable behaviour over such long time range.

The analysis of the spatial overlap between estimates from the 0° longitude and IODC orbit positions shows a very good agreement among the three individual satellite data records (MFG 0°, MSG 0°and MFG IODC 63° longitude). The correlation between the estimates is close to 0.99 and the RMSE is around 7%.

The validation sites are included in the list of sites of the Surface Albedo Validation Sites (SAVS)[2] [RD11]:

SITE NAME	LAT	LON	SURFACE TYPE
LIBIA_00001	27.4742	16.276	Bare soil
EGYPT_ONE	27.12	26.1	Bare soil
MORZUQ_DESERT	12.5	24.75	Bare soil
SOV	24.91	46.41	Bare soil
MONGU	-15.2536	23.1508	Urban
SKUKUZA	-25.02	31.4834	Shrubland
BELMANIP_00027	-11.0438	-39.9664	Vegetation

Table 5: SAVS site used for comparison with reference data. Latitude and Longitude are given in decimal degrees.

The validation against estimates from the MODIS instrument and the SAFARI campaign data shows a good agreement with DHR30 RMSE values always between 2% and 7% for bright desert sites and around 8% for the MONGU site. The worst agreement is for BELMANIP_00025 where the RMSE value is 8.9%. As demonstrated above, the introduction of an external cloud mask improved significantly the quality of the retrieval. Anyway, detection of clouds with the current method is more difficult at high satellite viewing zenith angles (longer path through the atmosphere), in particular over regions with permanent cloud overcast. A possible improvement to overcome this limitation and to further remove the minimal remaining cloud contamination in the retrieved albedo data record is to follow the approach presented in [RD13]. This method creates climatological seasonal background (cloud free) albedo from the GSA data record itself. The usage of an external climatological value, depending on a different aerosol retrieval, could introduce albedo variations due to a different estimation of the coupled albedo-aerosol system that might be taken as real changes. The retrieved DHR30 is compared against the climatological background and values 40% higher should be removed. This approach could have a negative impact on snow covered single pixels, removing sporadic snow falls and should then carefully considered according to the user's objective.

4.3 Limitations in usage

The GSA retrieval scheme can be applied to a wide set of geostationary satellites ([RD15] and [RD10]). It has been developed to exploit imagery acquired by old imagers having an extremely limited spectral radiometric capacity. The drawback is the introduction of limitations in the quality of the retrieval. GSA attempts to mitigate the impact of such limitations providing the user with some control parameters such as uncertainty estimates and the probability (being an index for the goodness of the solution of the retrieval problem) in the set of albedo estimates over 10 days at one location.

[2] DOI: http://dx.doi.org/10.15770/EUM_SEC_CLM_1001

The radiometer on board the MFG and MSG satellites acquires radiances twice (four times) per hour in a single broad solar spectral band ranging from 0.4 µm up to 1.1 µm (see Figure 2). This spectral interval contains some gas absorption bands and is subject to aerosol scattering-absorption processes whose magnitude depends on the wavelength. Because of this, the decoupling between absorption and scattering processes done in the retrieval introduces uncertainty due to the integration over such a large spectral interval. Vegetation reflectance exhibits strong and fast variations over the spectral region 0.4 µm - 1.1 µm because of the differences in the radiation transfer regimes occurring on both sides of 0.7 µm. This is mainly driven by absorption at wavelengths shorter than 0.7 µm and by scattering at larger wavelengths. These spectral variations cannot be explicitly considered in the atmospheric-correction scheme because observations occur only in one single band. Consequently, the surface albedo estimates derived from geostationary satellite observations in the VIS band with the GSA algorithm are subject to systematic biases depending on the shape of the surface spectra, the aerosol load, and the absorbing gas concentration.

A further limitation for estimates from the SEVIRI instruments onboard the Meteosat Second Generation satellites is caused by the change of the instrument scanning mode during the time of operations. From 31 August 2005 onwards, the lower spatial coverage window of the HRV channel is shifting to follow the daily illumination by the sun, while it was fixed over Africa before this date. For this reason, for periods before 31/08/2005, no retrieval of South America is possible using the SEVIRI HRV images.

At high viewing zenith angles (far from the sub-satellite point), the geostationary projection introduces a distortion in the pixels and the path through the atmosphere is longer. The combination of these factors implies a lower reliability in both the cloud detection and albedo retrieval. The uncertainty and associated probability estimated at pixel level try to account for that. The user should pay particular attention when using the data from those areas. This effect is more relevant in case of areas subject to an on average high cloud cover like over Amazonia.

The range of variation allowed for the Aerosol Optical Thickness (AOD) in the look-up tables (see Table 6) might lead to a higher albedo due to the saturation of the aerosol contribution (AOD > 1) in the coupled system. The analysis of the AOD has been addressed for Release 1 [AD1] and it is valid for Release 2.

No atmospheric correction is performed depending on the pixel elevation. This can lead to an underestimation of the coupled surface-aerosol system because the air column is thinner than assumed. However, this will only affect areas like the Himalaya region or the highland in South Africa.

5 DATA RECORD GENERATION

A complete and detailed mathematical description of the retrieval algorithm is given in the Algorithm Theoretical Basis Document (ATBD) [AD2]. The algorithm is based on a method proposed by Pinty et al. ([RD5] and [RD6]) to retrieve the surface anisotropy and the atmospheric aerosol load through the inversion of a Radiative Transfer Model (RTM) and the accumulation of geostationary cloud free observations acquired in the visible part of the electromagnetic spectrum at different illumination conditions (see Figure 9). This retrieval scheme relies on the applicability of the reciprocity principle at a spatial scale of several kilometres [RD3]. According to this principle, measurements taken at different viewing angles correspond to similar measurements at different

sun illumination conditions. Assuming that the geophysical properties controlling the radiance field emerging from a given pixel do not evolve much over a day, the acquisition of radiance data over such a period corresponds to an angular sampling of the same radiance field for various solar geometries.

The usage of Meteosat VIS data only cannot guarantee a robust and accurate retrieval. To further constrain the retrieval problem to the surface–aerosol system only, the atmospheric state is characterised ingesting ERA-Interim reanalysis Total Column Ozone (TCO3) and Total Column Water Vapour (TCWV) produced at the European Centre for Medium-Range Weather Forecasts (ECMWF) [RD12]. The lack of spectral information and the radiometric noise limit the possibility to discriminate unequivocally among the various solutions that could fit the measurement vector (Top of Atmosphere BRF) at a given level of confidence. This level of confidence depends on the size of the measurement vector that can change from pixel to pixel according to cloud and illumination conditions and to possible gaps in the input satellite images. Hence, a probability is assigned to each solution. This probability specifically depends on the number of degrees of freedom and the value of the cost function.

τ aerosol optical depth @ 550 nm	0.1, 0.2, 0.3, 0.4, 0.6, 0.8, 1.0
k parameter	0.4, 0.5, 0.6, 0.7, 0.8, 0.9, 1.0
Θ parameter	-0.30, -0.25, -0.20, -0.15, -0.10, -0.05, 0.00

Table 6: RPV Radiative Transfer Model parameters. The inversion is performed on pre-computed LUT using these values to speed-up the retrieval.

The most critical variables of such a system are then the aerosol optical-depth and the surface brightness. It is assumed that actual aerosol situation matches one of the limited numbers of standard atmospheric models which can be prescribed from experience (parameter τ in Table 6), The surface brightness is estimated during the same retrieval process from a set of predefined solutions (parameters k, Θ in Table 6) which describe the anisotropic properties of typical surfaces. The reflectance level ρ_0 is an unconstrained parameter. The approach followed in solving this surface-aerosol scattering problem is an extension of the MISR algorithm for retrieving aerosol optical depth values over dark surfaces [RD14].

The algorithm also estimates the retrieval parameter error relying on a statistical analysis of the solution ensemble that satisfies the inversion scheme given the measurement uncertainty (for details refer to [RD4]). A 10-day temporal compositing technique is applied to maximise the spatial coverage of cloud-free pixels. Finally, the retrieved surface state variables are used to derive the Directional Hemispherical Reflectance (DHR) corresponding to a sun position of 30 ° together with its respective error. The estimated retrieval uncertainty and the probability of the solution are the two key elements that permit a meaningful comparison of surface albedo derived from different radiometers.

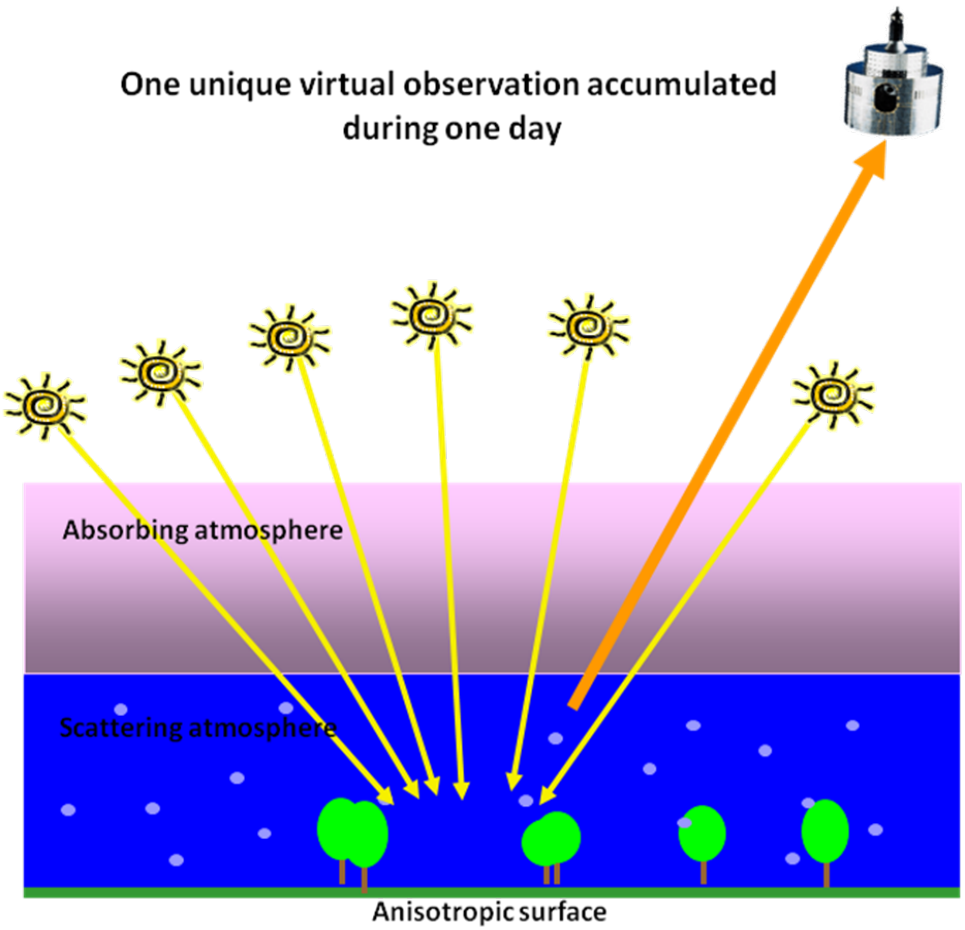

Figure 9: GSA Retrieval scheme. The observations accumulated during the day are used as an angular sampling of the surface.

Due to the huge amount of calculations needed, in particular for the generation of a many decades long data record, the number of possible states of the coupled surface-aerosol system is limited to a fixed number (see Table 6). The usage of pre-calculated Look-Up Tables (LUT) speeds up the per pixel base retrieval. The algorithm also estimates retrieval uncertainty and provides a probability for the retrieval [RD4] calculated according to the quality of the fit and the actual number of available observations. The retrieval is performed using the spectral instrument visible channel for MVIRI (Meteosat-2 to Meteosat-7) and in the High-Resolution Visible (HRV) channel for SEVIRI (Meteosat-8 to Meteosat-10). The product contains also the uncertainties and other ancillary information. Figure 10 shows the spectral bands for the individual instruments giving an indication how diverse they are. In the retrieval process, it is assumed that the SSRs do not change in time and are not affected by any uncertainty. In order to make the albedo estimates comparable and enable comparison with other surface albedo data records, e.g., the MODIS data record used as a reference, the albedo quantities retrieved with GSA need to be converted into a broadband spectral interval (0.3-3.0 µm). This conversion to broadband is explained in details in Section 3.3.

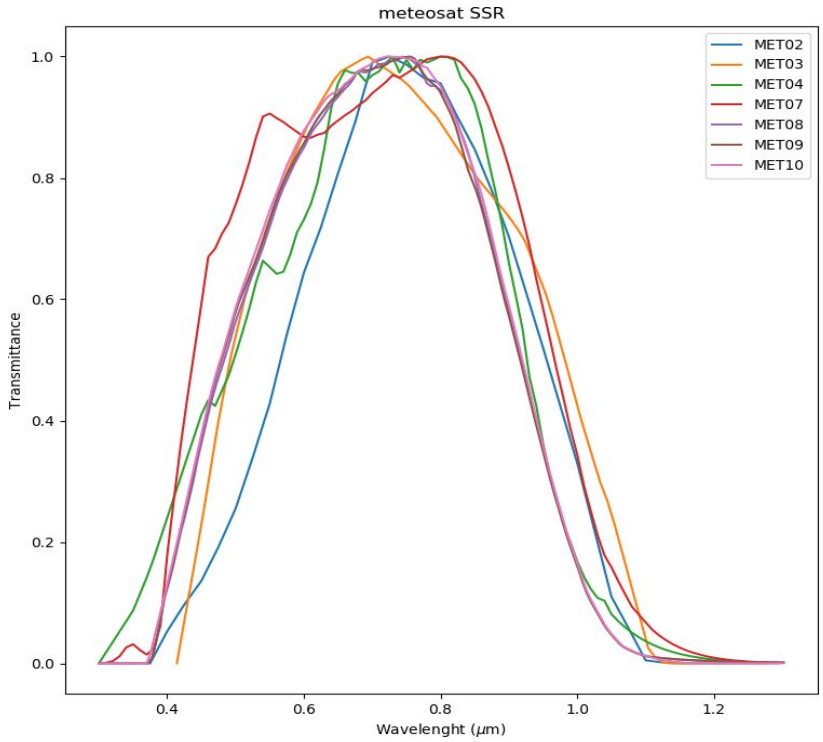

Figure 10: Sensor Spectral Responses (SSRs) for the VIS (HRV) band of the MVIRI (SEVIRI) instruments

5.1 Input Data

The input data for the GSA algorithm are divided into two classes: dynamic (see Table 7) and static (see Table 8). In the class of the dynamic input there are: Meteosat imagery, Cloud Mask, Re-analysis data. Static input data are: Look-Up Tables for the model inversion, Latitude/Longitude information.

5.1.1 Meteosat Imagery

This release contains products generated with imagery acquired by both MVIRI and SEVIRI instruments. MVIRI is the Meteosat Visible Infra-Red Imager instrument that was operated on-board EUMETSAT's Meteosat First Generation (MFG) series of European geostationary satellites during the years 1977 – 2017. The MFG series consisted of seven satellites. The first MFG satellite (Meteosat-1) was launched in 1977 but failed in late 1979. Meteosat-2 took up operations in late 1982 and since then an unbroken data record exists.

SEVIRI is the Spinning Enhanced Visible and Infra-Red Imager instrument that is operated on-board EUMETSAT's Meteosat Second Generation (MSG) series of European geostationary satellites as of 2004. The MSG series consists of four satellites and the first MSG satellite (Meteosat-8) was launched in August 2002. This release contains products generated at 0° for Meteosat-8, 9, 10 (Figure 11).

All Meteosat positions over the Indian Ocean, irrespective of the satellite generation, are part of the IODC data service established to support the international Indian Ocean Experiment (INDOEX) in 1998. For this purpose, Meteosat-5 was moved to a position at 63°E and started its operational service on 1 July 1998. Due to its scientific relevance, the service was continued with Meteosat-7 at 57°E from December 2006 onwards.

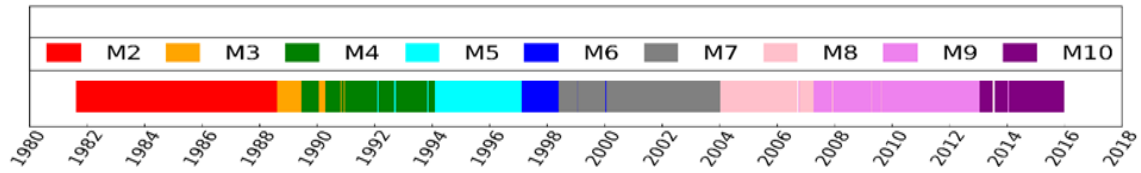

Figure 11: Operational Meteosat prime satellite over the period.

5.1.2 Cloud Mask

The Cloud Mask is retrieved for both MVIRI and SEVIRI using the same algorithm developed at MeteoSwiss, within the Climate Monitoring SAF [RD7]. The implemented scheme is based on a Bayesian approach applied to a set of scores calculated exploiting only the two visible SEVIRI channels (one single visible channel for MVIRI) and the thermal IR channel around 10.8 µm. The algorithm also builds up a daily background reflectance map to assess potential clouds with higher reliability. The mask is provided as a Cloud Fractional Cover (CFC) in eight steps from zero to 100%. Only pixels with CFC=0 are considered for processing.

5.1.3 Re-analysis Data

The ECMWF ERA-interim reanalysis [RD12], the Total Column Ozone (TCO3) and Total Column Water Vapour (TCWV) are used in one of the Look-Up Tables (LUT) in order to invert the Radiative Transfer Model (RTM). Several ozone and water vapour bands are located within the Meteosat visible spectral response and the effects of these gases on radiation transfer processes must be considered. The sensitivity of the proposed retrieval schemes with respect to those atmospheric parameters has been analysed in [AD2].

File	Meaning	Units
Radiance	Radiance at pixel resolution in the instrument visible band	Wm^{-2} sr^{-1}
Cloud Mask	Cloud mask at pixel level. If not present, the algorithm assumes all pixels are cloud-free. 0: Cloud free 1: Cloudy	1
NWP Model Reanalysis Data	Total Column Ozone (TCO3) and Total Column Water Vapour (TCWV). If not present, default values are used: TCO3 : 0.3cm atm TCWV : 2.0 gcm^{-2}	TCO3: cm atm TCWV: gcm^{-2}

Table 7: GSA dynamic input files

File	Meaning
Look Up Table (LUT)	Binary files. The LUTs contains pre-computed integrals used for the RTM inversion
Latitude	MVIR/SEVIRII rectified image
Longitude	MVIRI/SEVIRI rectified image

Table 8: Ancillary files GSA static input

5.2 Data Processing Strategy

The processing consists of three parts (see Figure 12):

(1) GSA::Cloud Mask: The Cloud Mask is generated for both MVIRI and SEVIRI using the same algorithm developed at MeteoSwiss within the Climate Monitoring SAF [RD7]. The implemented scheme is based on a Bayesian approach applied to a set of scores calculated exploiting only the two visible SEVIRI channels (one single visible channel for MVIRI) and the thermal IR channel around 10.8 µm. The algorithm also builds up a daily background reflectance map to assess potential clouds with higher reliability. The mask is provided as a Cloud Fractional Cover (CFC) in 8 steps from 0 to 100%. Only pixels with a CFC=0 are used because considered as cloud free.

(2) GSA::Acceptor: The native input 1.5 data in the native instrument-specific format are converted into a unique format, valid for any instruments. Information about calibration, radiometric quality and others are also included in this format.

(3) GSA::Retrieval: Generate 10-day albedo records as described in [AD2].

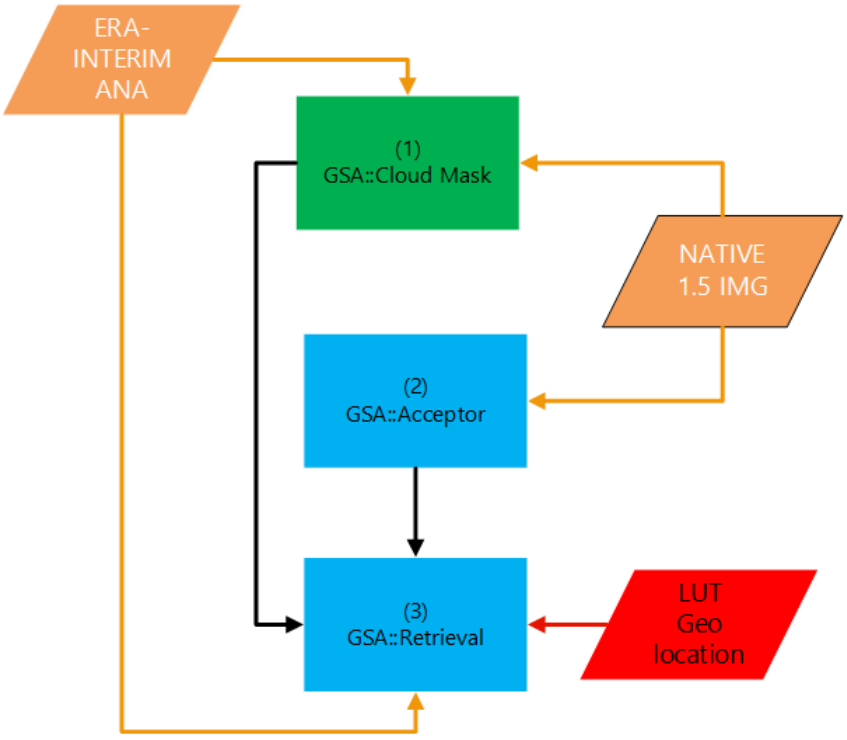

Figure 12: GSA processing steps.

5.3 Processing Outline

The GSA algorithm is organised into two main processing steps, responsible respectively for the daily accumulation of the required input data and for the retrieval. The accumulation and retrieval is performed dividing the processing area into small geographical area called *windows*. The windows for the 0-degree (MFG and MSG), 057-degree and 063-degree missions are shown in Figure 13.

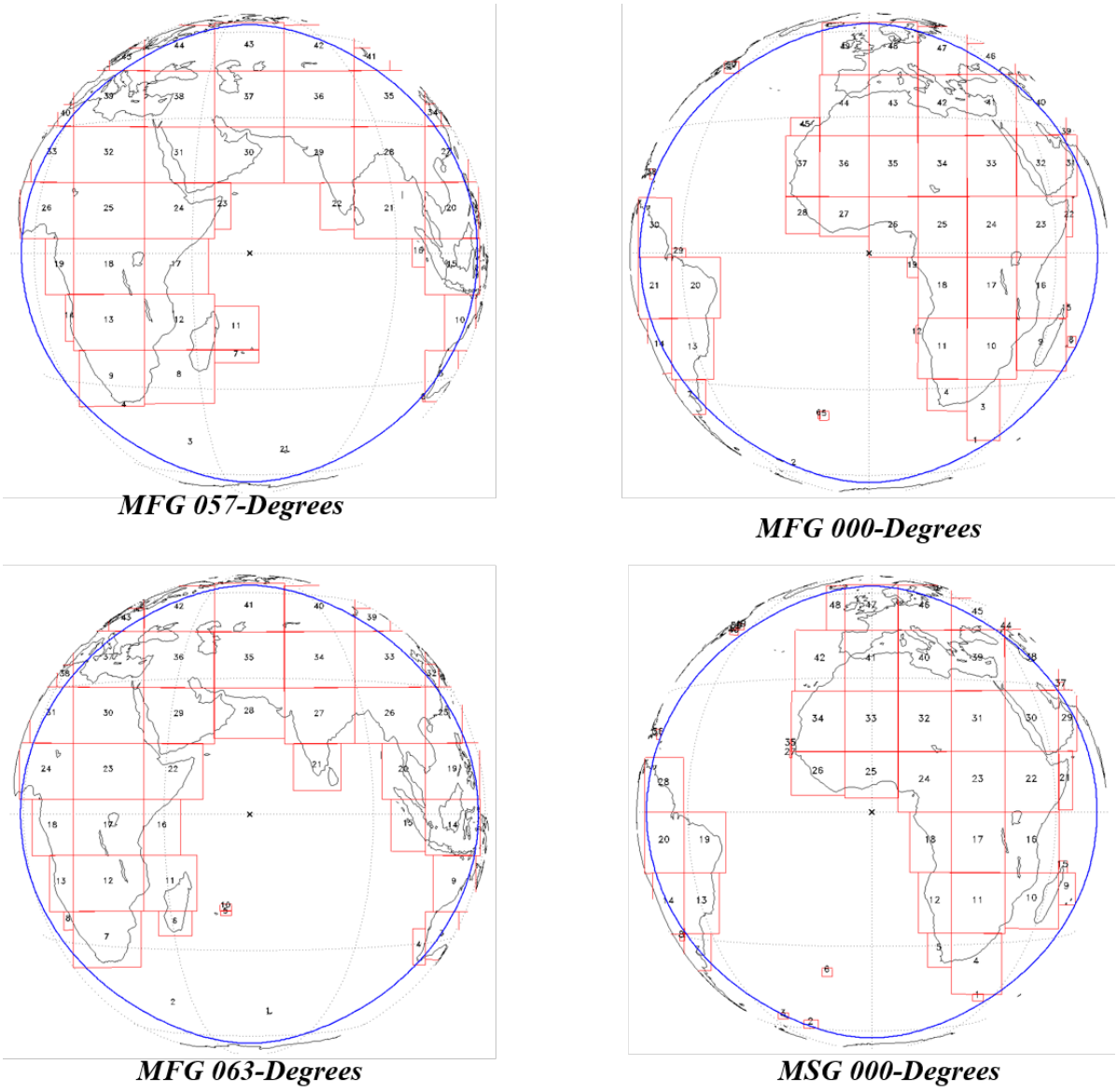

Figure 13: Illustration of the processing windows.

In the first part of the processing, called Data Accumulation Module (DAM), the TOA measurements for each pixel in each *window* are stored in files called Data Accumulation Module (DAM) files together with any other dynamical or static ancillary information needed for the retrieval.

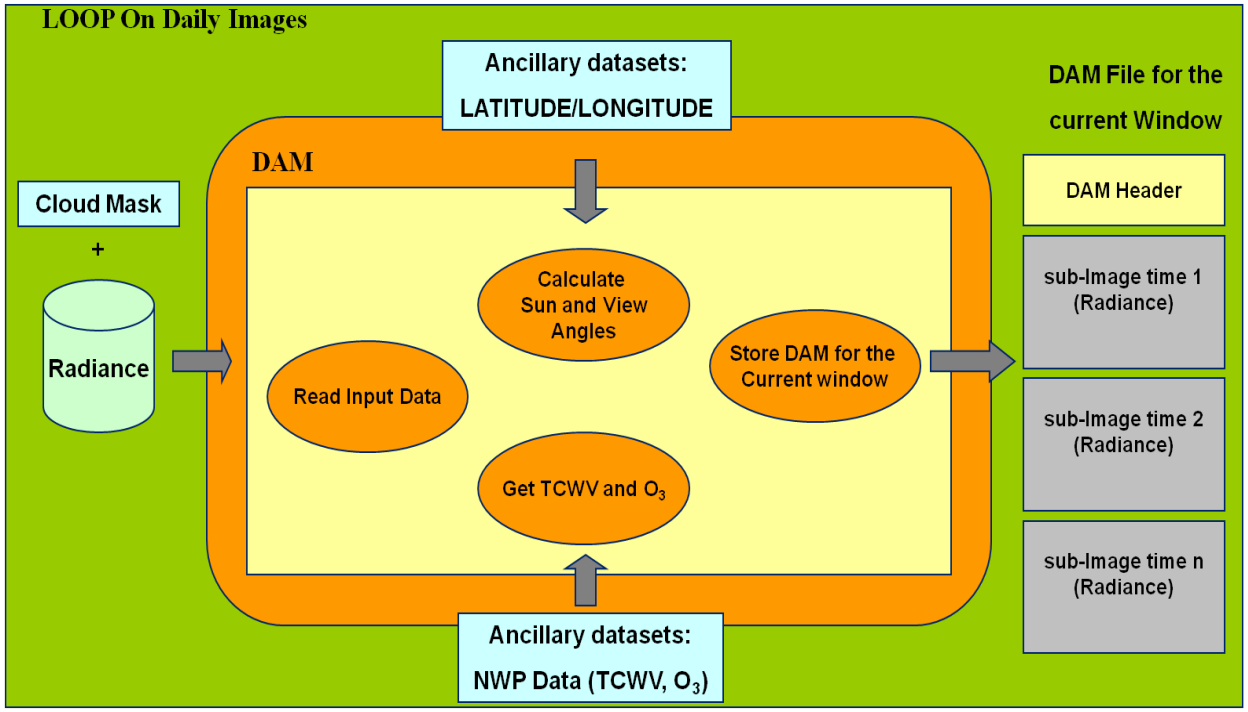

Figure 14: Daily Accumulation Model (DAM): functionalities and interface

The retrieval is performed in the second step, the Data Processing Module (DPM), after the daily accumulation of the cloud free observations. To speed up the retrieval, the field of solutions for the RTM is discretized (see Table 6) and all the necessary integrals for of the radiative transfer equations are stored in Look-up Tables has detailed specifications. After a solution for each pixel in each *window* is determined, the retrieval information is stored in the Space Averaging Module (SAM) files. Finally, among all the solutions retrieved for the 10-day period, one is selected and stored in the final product [AD2].

This retrieval approach is implemented in the following four steps in the DPM:

Before proceeding with the retrieval, two thresholds are applied to the accumulated TOA BRF and measurements with a value below 0.05 and greater than 0.6 are excluded.

1. **Data Consistency Procedure (DCP):** This module is responsible for screening out the not cloud-free pixels and it must be executed before entering the Atmospheric Scattering Module. This procedure runs for every pixel. If a cloud mask is available (optional input), it is applied prior to the DCP process. In this case only pixels with a CFC=0 are provided as input.

2. **Atmospheric Scattering Module (ASM):** In this module, the gas absorption contribution to the Top of Atmosphere reflectance is removed and the inversion of the RTM representing the scattering layer and surface reflectance for all the possible values of the parameterised fields (values in Table 6) is performed.

3. **Data Interpretation Module (DIM):** In this module, the most likely solution among all the possible ones estimated in the previous step for each pixel is chosen [AD2].

4. **Space-Time Averaging Module (TAM):** Steps 1 to 3 are applied after the daily accumulation and the solutions stored in the SAM temporary files for the subsequent 10-day temporal compositing. In this latter module, the best solution for the 10-day period is selected [AD2].

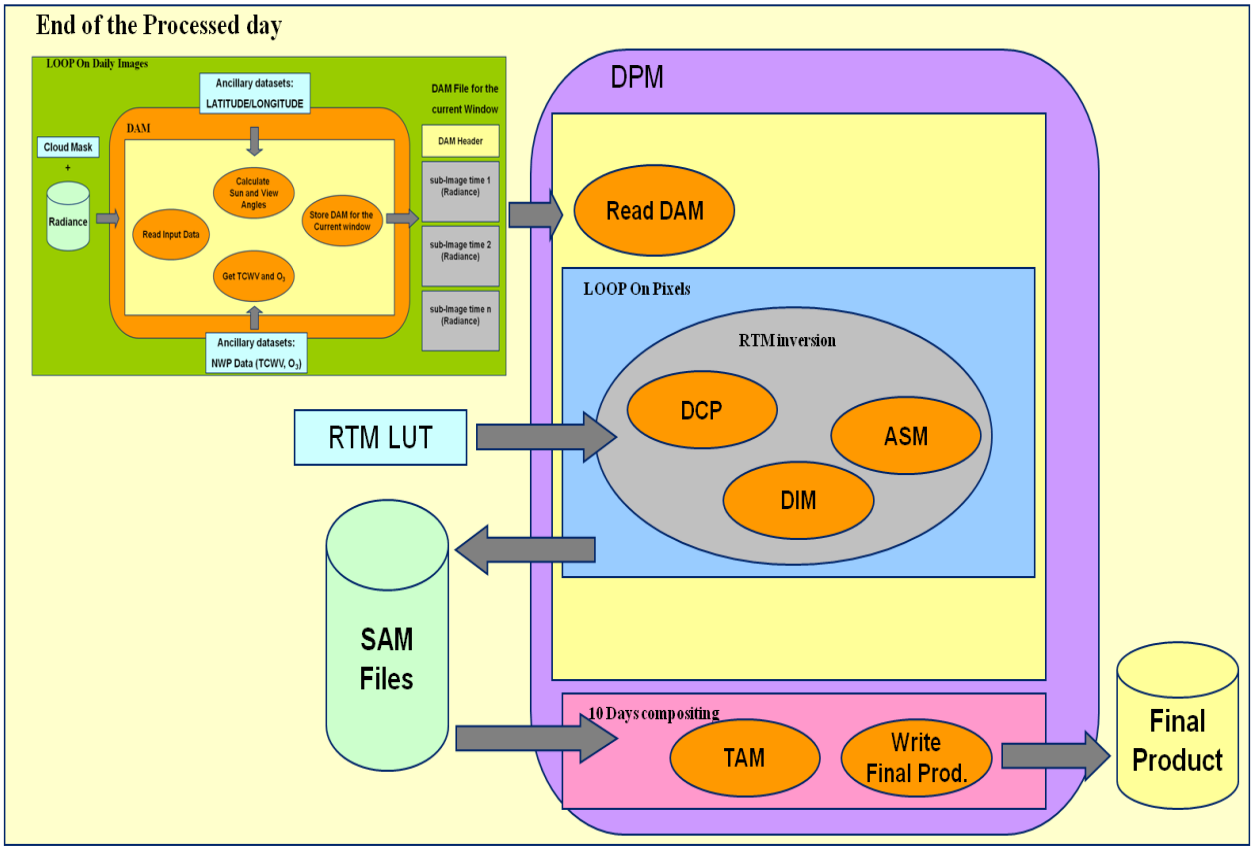

Figure 15: Data Processing Module (DPM): functionalities and interface

6 PRODUCT FORMAT DESCRIPTION

6.1 Overview

The products are provided in NetCDF4[3] format. They consist of a set of global attributes and an ensemble of 23 variables. The geolocation is not included in the products but is made available to the users as an external ancillary file, one for each satellite platform and sub-satellite point. One GSA product contains surface albedo estimates derived from the Meteosat VIS band spectral range. One product generated every 10-day compositing periods. These compositing periods are defined by the Julian day number. The first period runs from day 1 to day 10, the second from day 11 to day 20, and so on. The last period of the year is therefore slightly shorter than the other periods and runs from day 361 to 365 (or to day 366 in a leap year). There is a maximum of 37 products per year. The GSA product is not derived over the entire Meteosat disk and no sea mask is applied during the generation process so that values over sea are also available is this area but they should not be considered for any applications.

The spatial resolution at sub-satellite point is:

[3] https://www.unidata.ucar.edu/software/netcdf/ Link valid 09/04/2020

- MVIRI: 2.5 km
- SEVIRI[4] 3 km

6.1.1 Naming convention

The GSA product filename follows the WMO convention adopted in EUMETSAT for NetCDF files [AD4]:

W_XX-EUMETSAT-Darmstadt,SURFACE+SAT,<SATID>+<INSTRUMENT>+GSA_C_<ORIGINATOR>_<START_DATE>_<END_DATE>_1_OR_FES_<SSP>_0200.nc

	MFG	**MSG**
SATID	MET02,...,MET07	MET08,…,MET10
INSTRUMENT	MVIRI	SEVIRI
ORIGINATOR	EUMS	EUMG
START_DATE	yyyyMMddhhmmss	yyyyMMddhhmmss
END_DATE	yyyyMMddhhmmss	yyyyMMddhhmmss
SSP	E0000, E0570, E0630	E0000

Table 9: GSA filename description

Each product covers a period of 10 days.

6.1.2 Global attributes

The table on the two pages that follow contains all the global attributes for the GSA product file.

Attribute	**Description**
id	DOI for this product
processing_algorithm_version	Processing algorithm version.
day_in_year_start	Starting day of the year of the compositing period.
day_in_year_end	Ending day of the year of the compositing period.
year	Year
time_coverage_start	Start date and time of the product temporal coverage
time_coverage_end	End date and time of the product temporal coverage
processing_mode	R for reprocessing
disposition_mode	O for Operational
nominal_ssp_longitude	Centre of the reference grid in the Meteosat projection.
geospatial_lat_min	lower latitude of the processed box
geospatial_lat_max	upper latitude of the processed box
geospatial_lon_min	more western longitude of the processed box
geospatial_lon_max	more eastern longitude of the processed box
data_created	Date and time when the NetCDF has been generated.
satellite_number	Number of the satellite in the platform series
operational_name	Satellite operational standard name
source	Product input type
num_valid_pixels	The total number of valid pixels in each data set.
num_proc_days	The actual number of days in the compositing period
calibration_source	Source of the calibration datasets.

[4] SEVIRI HRV sampling distance at Sub-satellite Point is 1 km. The input is rescaled as a 3x3 pixels to 3 km

product_version	Product release
institution	Institution of data generation
keywords	Relevant keywords defining the product content
summary	Short text describing the content of the product
creator_name	Name of the team responsible for the generation of the product
creator_email	Email of the product creator
creator_url	URL of the product creator
time_coverage_duration	Time period covered by the product
Conventions	CF conventions applied
naming_authority	Name of the product authority
licence	Licence for product usage
standard_name_vocabulary	CF standard name vocabulary
instrument	Satellite instrument used
platform	Meteosat first or Second Generation
water_refl_threshold	Minimum accepted TOA BRF for measurements
cloud_for_sure_threshold	Maximum TOA BRF BRF for measurements
perc_valid_pixels	Percentage of pixels with a valid solution among the total number of processed pixels.
avg_radiometric_err	Mean relative radiometric error (Equation 5) in per cent.
avg_available_slots	Mean number of available observation per pixel prior to the cloud screening.
avg_processed_slots	Mean value of N_y, the size of the measurement vector y_m.
avg_valid_pixels	Percentage of valid pixels.
avg_num_weak_sol	Percentage of pixels with a probability between 10 % and 50 %.
avg_num_dubious_sol	Percentage of pixels with a probability smaller than 10 %.
avg_solutions	Average number of solutions for each pixel
avg_tau	Mean optical thickness.
avg_probability	Mean value of the threshold probability.
avg_dhr30	Mean value of the DHR.
avg_dhr30_err	Mean value of the DHR error.
prob_num_val	Number of possible threshold probabilities
probability_values	Threshold probabilities
tau_num_val	Number of possible AOT values in the Look-Up Tables
optical_thickness	AOT values
k_num_val	Number of possible k values in the Look-Up Tables
k_values	K values
theta_num_val	Number of possible theta values in the Look-Up Tables
theta_values	Theta values

Table 10: Global attributes: GSA product file

SurfaceIndex	Θ	k	SurfaceIndex	Θ	k
0	-0.30	0.40	25	-0.15	0.80
1	-0.30	0.50	26	-0.15	0.90
2	-0.30	0.60	27	-0.15	1.00
3	-0.30	0.70	28	-0.10	0.40
4	-0.30	0.80	29	-0.10	0.50
5	-0.30	0.90	30	-0.10	0.60
6	-0.30	1.00	31	-0.10	0.70
7	-0.25	0.40	32	-0.10	0.80
8	-0.25	0.50	33	-0.10	0.90
9	-0.25	0.60	34	-0.10	1.00
10	-0.25	0.70	35	-0.05	0.40
11	-0.25	0.80	36	-0.05	0.50
12	-0.25	0.90	37	-0.05	0.60
13	-0.25	1.00	38	-0.05	0.70
14	-0.20	0.40	39	-0.05	0.80
15	-0.20	0.50	40	-0.05	0.90
16	-0.20	0.60	41	-0.05	1.00
17	-0.20	0.70	*42*	0.00	0.40
18	-0.20	0.80	*43*	0.00	0.50
19	-0.20	0.90	44	0.00	0.60
20	-0.20	1.00	45	0.00	0.70
21	-0.15	0.40	46	0.00	0.80
22	-0.15	0.50	47	0.00	0.90
23	-0.15	0.60	48	0.00	1.00
24	-0.15	0.70			

Table 11: (k, Θ) values according to the SurfaceIndex variable.

6.1.3 Variables

Each variable is a bi-dimensional matrix of pixels corresponding to an image in the Meteosat projection with the same east-west and south-north scanning mode (first pixel is southeast). These values are coded on one byte with the value 255 used to indicate invalid pixels. Decoded values are calculated as with DV = scale_factor × CV where DV is the decoded value and CV is encoded value. The scale_factor value is available as dataset attribute. . The fill value attribute for non-processed pixels is defined for all variables. The user is reminded that the albedo (DHR30 and BHRiso) and the DHR30 uncertainty are provided in the native VIS (HRV) band of MFG (MSG). Native to broadband correction is provided in Section 3.3.

The conversion from ***SurfaceIndex*** to the corresponding RPV model parameters (k, Θ) can be done according to Table 11.

The conversion from ***ProbabilityThreshold*** index to the provability value can be done using the values stored in the global attribute ***probability_values***.

The conversion from ***AOT*** index to the provability value can be done using the values stored in the global attribute ***theta_values***.

Name	Description
BHRiso	The isotropic Bi-Hemispherical Reflectance field contains the surface albedo that would have been observed under isotropic illumination conditions
DHR30	The Directional Hemispherical Reflectance field contains the surface albedo assuming a sun zenith angle of $\mu_0 = 30°$ observed with direct illumination only
DHR30_Error_10_Days	This field represents the estimated DHR30 error over 10 days.
ProbabilityThreshold	This field contains the probability threshold of the best solution day. Pixels with a probability smaller than 80% should be considered carefully. Pixels with very low probability (<50%) are flagged in the OverallQuality field.
OverallQuality	This flag takes the following values: **Value Meaning** 0 OK (realistic solution found) 1 No valid days in the period (no retrieval over the period) 2 No valid samples in the period (no valid solutions over the period) 3 No likely day (no realistic solutions) 4 Invalid solution index (index negative or higher than number of solutions) 5 Dubious solution (best solution Probability = 10%) 6 Weak solution (best solution Probability between 10% and 50%)
NumSolutions	The number of acceptable solutions. The value 255 is set for invalid pixels.
InputSlots	Number of inputs lots before cloud screening.
InputSlotsASM	Number of clear sky input slots.
SurfaceIndex	Index defining the couple (k, Θ) describing the shape of the surface BRF in the RPV model for the best fit (see Table 11).
AOT	Estimated equivalent aerosol optical thickness.
R_0	Amplitude of the surface BRF in the RPV model for best fit.
Error_R_0	Estimated uncertainty of R0
DaysAvailable	Number of days with a solution
BestDay	Selected day during the compositing period.
Chi2DCP	Cost function of the cloud screening in the DCP module.
Chi2ASM	Cost function of the inversion in the ASM module.
DHR30_Error_BestDay	Estimated uncertainty of the DHR for the best day d.
Error_K	Estimated uncertainty of the K RPV model parameter
Error_T	Estimated uncertainty of the Θ RPV model parameter
Error_Tau	Estimated uncertainty of AOT
AOTAvgValue	Average AOT value during the compositing period.
StdErrAOTAvgValue	Standard deviation of AVGOPT.
Radiom_RelError	Mean daily radiometric noise of the best day
latitude	Pixel latitude in degrees (S-N)
longitude	Pixel longitude in degrees (E-W)

Table 12: Name and description of the variables.

7 PRODUCT ORDERING

The data are accessible via the EUMETSAT Data Centre. To access the data from EUMETSAT, you need to register with the EUMETSAT Data Centre. When registered, you can order the data through a written request send to EUMETSAT's helpdesk.

7.1 Register with EUMETSAT Data Centre

Do this to register with the EUMETSAT Data Centre:

1. Register in the EUMETSAT EO-Portal (https://eoportal.eumetsat.int/) by clicking on the New User – Create New Account tab;
2. After finalisation of the registration process, an e-mail is sent to the e-mail address entered in the registration. Click the confirmation link in the e-mail to activate your account;
3. Login and subscribe to the Data Centre Service by going to the Service Subscription Tab and selecting Data Centre Service. Follow instructions issued from the web page to add needed information.

7.2 Order data

The data record described in this product user guide can also be ordered via the EUMETSAT User Service Helpdesk in Darmstadt, Germany. Please send a written request to this helpdesk, email ops@eumetsat.int, indicating the data record that you want to order including its Digital Object Identifier (DOI) number.

8 PRODUCT SUPPORT AND FEEDBACK

For enquiries about the GSA CDR described in this product user guide, please contact the EUMETSAT User Service Helpdesk by email: *ops@eumetsat.int.*

9 PRODUCT REFERENCING

The data record described in this product user guide has a unique DOI that should be used for referencing. The product's filename provides a unique identifier for each product.

APPENDIX A DATA RECORD AVAILABILITY

In the following plots the availability of the 10-day products is presented, together with the data record gaps. The gaps are due to missing input images. As described in the ATBD [AD2], a minimum number of six cloud-free measurements is necessary for the model inversion and albedo retrieval. In the following plots, the gaps for the 10-day period products are shown. Missing products are in red (value 0), while periods where two products are available (from different platform) are plotted in blue (value 2). Green means that one single product is available (value 1).

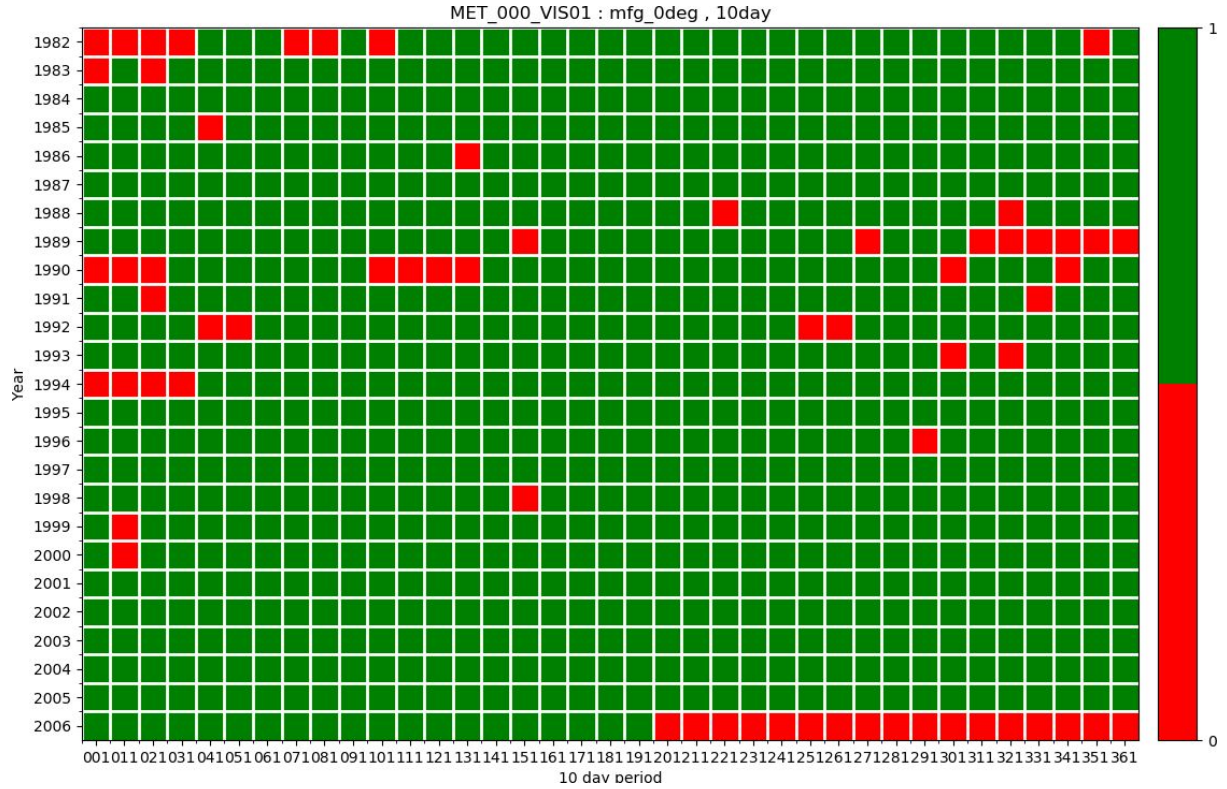

Figure 16: Gaps for the processing of MFG 0-degree mission.

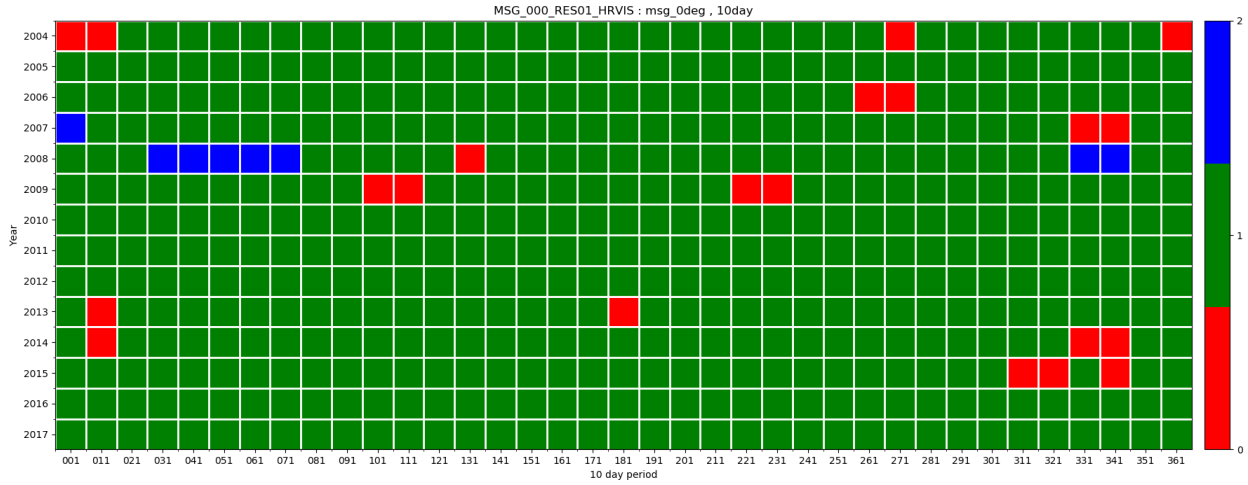

Figure 17: Gaps for the processing of MSG 0-degree mission.

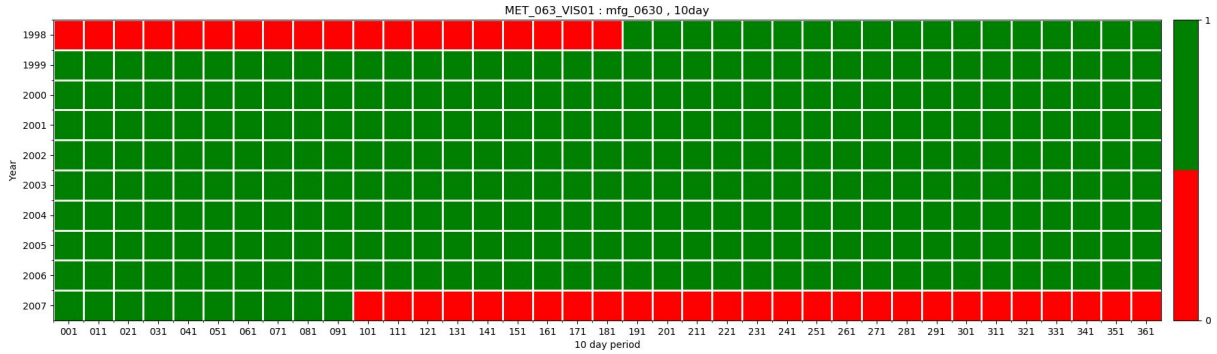

Figure 18: Gaps for the processing of Meteosat-5 63-degree mission.

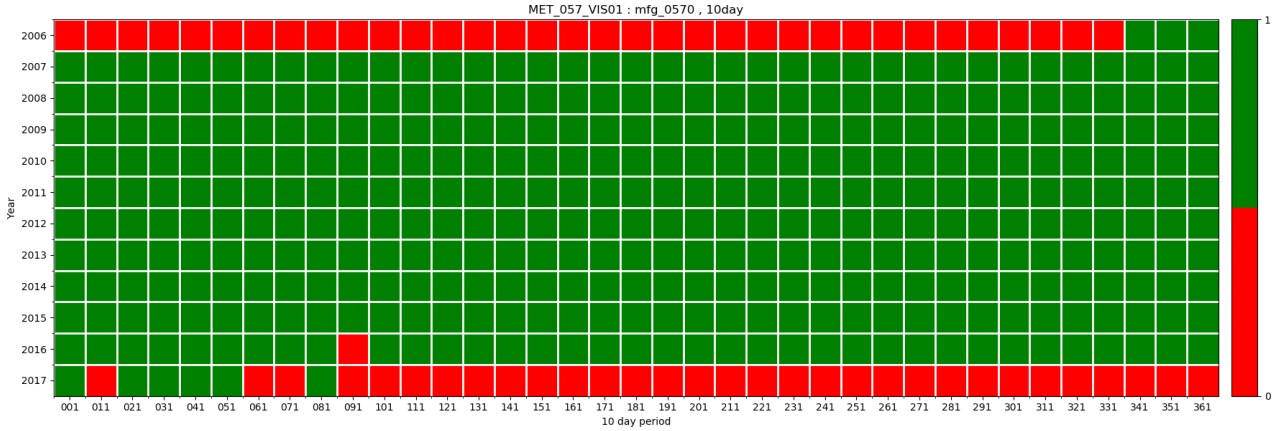

Figure 19: Gaps for the processing of Meteosat-7 57-degree mission.